augmentation or reconstruction and mega volume (>200 mL) fat grafting for primary breast augmentation, breast reconstruction, and gluteal augmentation. Clinically, certain type of surgical instruments or equipment also need to be studied so that plastic surgeons will use better and more reliable instruments or equipment to perform small, large or mega volume fat grafting for their patients.

SUMMARY

Autologous fat grafting is an exciting field in plastic and reconstructive surgery. Fat serves as a filler as well as its role for tissue regeneration will likely play a more important role in our specialty. As we learn more about the basic science of fat grafting and the standardized techniques and instruments used for fat grafting, this procedure alone or in conjunction with some less invasive procedures may be able to replace many operations that we perform currently. The minimally invasive nature of the procedure will benefit greatly our cosmetic and reconstructive patients, and may even achieve better clinical outcomes. We live in this exciting time of plastic surgery and look forward to the new era of our specialty.

REFERENCES

1. Gutowski KA, ASPS Fat Graft Task Force. Current applications and safety of autologous fat grafts: a report of the ASPS fat graft task force. Plast Reconstr Surg 2009;124:272–80.
2. Gir P, Brown SA, Oni G, et al. Fat grafting: evidence-based review on autologous fat harvesting, processing, reinjection, and storage. Plast Reconstr Surg 2012;130:249–58.
3. Kling RE, Mehrara BJ, Pusic AL, et al. Trends in autologous fat grafting to the breast: a national survey of the American Society of Plastic Surgeons. Plast Reconstr Surg 2013;132:35–46.
4. Coleman SR. Structural fat grafting: more than a permanent filler. Plast Reconstr Surg 2006;118:108S–20S.
5. Mojallal A, Lequeux C, Shipkov C, et al. Improvement of skin quality after fat grating: clinical observation and an animal study. Plast Reconstr Surg 2009;124:765–74.
6. Rohrich RJ, Ghavami A, Constantine FC, et al. Lift-and-fill face lift: integrating the fat compartments. Plast Reconstr Surg 2014;133:756e–67e.
7. Erol OO. Microfat grafting in nasal surgery. Aesthet Surg J 2013;34:671–86.
8. Tanikawa DY, Aguena M, Bueno DF, et al. Fat grafts supplemented with adipose-derived stromal cells in the rehabilitation of patients with craniofacial microsomia. Plast Reconstr Surg 2013;132:141–52.
9. Tanna N, Wan DC, Kawamoto HK, et al. Craniofacial microsomia soft-tissue reconstruction comparison: inframammary extended circumflex scapular flap versus serial fat grafting. Plast Reconstr Surg 2011;127:802–11.
10. Phulpin B, Gangloff P, Tran N, et al. Rehabilitation of irradiated head and neck tissues by autologous fat transplantation. Plast Reconstr Surg 2013;132:141–52.
11. DeFatta RA, DeFatta RJ, Sataloff RT. Laryngeal lipotransfer: review of a 14-year experience. J Voice 2013;27:512–5.
12. Coleman SR, Saboeiro AP. Fat grafting to the breast revisited: safety and efficacy. Plast Reconstr Surg 2007;119:775–85.
13. Del Vecchio DA, Bucky LP. Breast augmentation using preexpansion and autologous fat transplantation: a clinical radiographic study. Plast Reconstr Surg 2011;127:2241–450.
14. Veber M, Tourasse C, Toussoun G, et al. Radiographic findings after breast augmentation by autologous fat transfer. Plast Reconstr Surg 2011;127:1289–99.
15. Khouri RK, Rigotti G, Cardoso E, et al. Megavolume autologous fat transfer: part I. Theory and principles. Plast Reconstr Surg 2014;133:550–7.
16. Khouri RK, Rigotti G, Cardoso E, et al. Megavolume autologous fat transfer: part II. Practice and techniques. Plast Reconstr Surg 2014;133:1369–77.
17. Khoobehi K, Sadeghi A. Single staged mastopexy with autologous fat grafting [Abstract]. Plast Reconstr Surg 2009;124(Suppl 4):8–9.
18. Del Vecchio DA. "SIEF" – Simultaneous implant exchange with fat: a new option in revision breast implant surgery. Plast Reconstr Surg 2012;130:1187–96.
19. Auclair E, Blondeel P, Alexander D, et al. Composite breast augmentation: soft-tissue planning using implants and fat. Plast Reconstr Surg 2013;132:558–68.
20. Delay E, Sinna R, Ho Quoc C. Tuberous breast correction by fat grafting. Aesthet Surg J 2012;33:522–8.
21. Ho Quoc C, Sinna R, Gourari A, et al. Percutaneous fasciotomies and fat grafting: indication for breast surgery. Aesthet Surg J 2013;34:671–86.
22. Kanchwala S, Glatt BS, Conant EF, et al. Autologous fat grafting to the reconstructed breast: the management of acquired contour deformities. Plast Reconstr Surg 2009;124:409–18.
23. Seth AK, Hirsch EM, Kim JY, et al. Long-term outcomes following fat grafting in prosthetic breast reconstruction: a comparative analysis. Plast Reconstr Surg 2012;130:984–90.
24. Serra-Renom JM, Munoz-Olmo JL, Serra-Mestre JM. Fat grafting in postmastectomy breast reconstruction with expanders and prostheses in patients who have received radiotherapy: formation of new

subcutaneous tissue. Plast Reconstr Surg 2010;125:12–8.
25. Salgarello M, Visconti G, Barone-Adesi L. Fat grafting and breast reconstruction with implant: another option for irradiated breast cancer patients. Plast Reconstr Surg 2010;129:317–29.
26. Khouri RK, Eisenmann-Klein M, Cardoso E, et al. Brava and autologous fat transfer is a safe and effective breast augmentation alternative: results of a 6-year, 81-patient, prospective multicenter study. Plast Reconstr Surg 2012;129:1173–87.
27. Uda H, Sugawara Y, Sarukawa S, et al. Brava and autologous fat grafting for breast reconstruction after cancer surgery. Plast Reconstr Surg 2014;133:203–13.
28. Khouri RK, Rigotti G, Khouri RK Jr, et al. Total breast reconstruction with autologous fat transfer: review of a seven-year multicenter experience. Plast Reconstr Surg 2014;134:84–5.
29. Serra F, Aboudib JH. Gluteal implant displacement: diagnosis and treatment. Plast Reconstr Surg 2014;134:647–54.
30. Murillo WL. Buttock augmentation: case studies of fat injection monitored by magnetic resonance imaging. Plast Reconstr Surg 2004;114:1606–14.
31. Cardenas-Camarena L, Arenas-Quintana R, Robles-Cervantes JA. Buttocks fat grafting: 14 years of evolution and experience. Plast Reconstr Surg 2011;128:545–55.
32. Coleman SR. Hand rejuvenation with structural fat grafting. Plast Reconstr Surg 2002;110:1731–44.
33. Rigotti G, Marchi A, Galie M, et al. Clinical treatment of radiotherapy tissue damage by lipoaspirate transplant: a healing process mediated by adipose-derived adult stem cells. Plast Reconstr Surg 2007;119:1409–22.
34. Del Vecchio D, Rohrich RJ. A classification of clinical fat grafting: different problems, different solutions. Plast Reconstr Surg 2012;130:511–22.
35. Khouri RK, Smit JM, Cardoso E, et al. Percutaneous aponeurotomy and lipofilling: a regenerative alternative to flap reconstruction? Plast Reconstr Surg 2013;132:1280–90.
36. Hovius SE, Kan HJ, Smit X, et al. Extensive percutaneous aponeurotomy and lipografting: a new treatment for Dupuytren disease. Plast Reconstr Surg 2011;128:221–8.
37. Bank J, Fuller SM, Henry GI, et al. Fat grafting to the hand in patients with Raynaud phenomenon: a novel therapeutic modality. Plast Reconstr Surg 2013;133:1109–18.
38. Mazzola IC, Cantarella G, Mazzola RF. Management of tracheostomy scar by autologous fat transplantation: a minimally invasive new approach. J Craniofac Surg 2013;24:1361–4.
39. Pallua N, Baroncini A, Alharbi Z, et al. Improvement of facial scar appearance and microcirculation by autologous lipofilling. J Plast Reconstr Aesthet Surg 2014;67:1033–7.
40. Caviggioli F, Maione L, Forcellini D, et al. Autologous fat graft in postmastectomy pain syndrome. Plast Reconstr Surg 2011;128:349–52.
41. Huang SH, Wu SH, Chang KP, et al. Autologous fat grafting alleviates burn-induced neuropathic pain in rats. Plast Reconstr Surg 2014;133:1396–405.
42. Yoshimura K, Sato K, Aoi N, et al. Cell-assisted lipotransfer for cosmetic breast augmentation: supportive use of adipose-derived stem/stromal cells. Aesthetic Plast Surg 2008;32:48–55.
43. Kolle SF, Fischer-Nielsen A, Mathiasen AB, et al. Enrichment of autologous fat grafts with ex-vivo expanded adipose tissue-derived stem cells for graft survival: a randomized placebo-controlled trial. Lancet 2013;382:1113–20.
44. Tonnard P, Verpaele A, Geert Peeters G, et al. Nanofat grafting: basic research and clinical applications. Plast Reconstr Surg 2013;132:1017–26.
45. Raposio E, Caruana G, Bonomini S, et al. Novel and effective strategy for the isolation of adipose-derived stem cells: minimally manipulated adipose- derived stem cells for more rapid and safe stem cell therapy. Plast Reconstr Surg 2014;133:1406–9.
46. Longaker MT, Aston SJ, Baker DC, et al. Fat transfer in 2014: what we do not know. Plast Reconstr Surg 2014;133:1305–7.
47. Zhao J, Yi C, Li L, et al. Observations on the survival and neovascularization of fat grafts interchanged between C57BL/6-gfp and C57BL/6 mice. Plast Reconstr Surg 2012;133:398e–406e.
48. Eto H, Kato H, Suga H, et al. The fate of adipocytes after nonvascularized fat grafting: evidence of early death and replacement of adipocytes. Plast Reconstr Surg 2012;129:1081–92.
49. Pu LL. Cryoperservation of adipose tissue. Organogenesis 2009;5:138–42.

Differential Contributions of Graft-Derived and Host-Derived Cells in Tissue Regeneration/ Remodeling after Fat Grafting

Kentaro Doi
Fusa Ogata
Hitomi Eto
Harunosuke Kato
Shinichiro Kuno
Kahori Kinoshita
Koji Kanayama
Jingwei Feng
Ichiro Manabe
Kotaro Yoshimura, M.D.

Tokyo, Japan

Background: Recent research indicates that the adipose tissue of nonvascularized grafts is completely remodeled within 3 months, although origins of next-generation cells are unclear.

Methods: Inguinal fat pads of green fluorescent protein mice and wild-type mice were cross-transplanted beneath the scalp. At 1, 2, 4, and 12 weeks after transplantation, grafted fat was harvested, weighed, and analyzed through immunohistochemistry, whole-mount staining, and flow cytometry of cell isolates. Bone marrow of green fluorescent protein mice was transplanted to wild-type mice (after irradiation). Eight weeks later, these mice also received fat grafts, which were analyzed as well.

Results: The majority of host-derived cells detected during remodeling of grafted fat were macrophages (>90 percent at the early stage; 60 percent at 12 weeks). Cell origins were analyzed at 12 weeks (i.e., when completely regenerated). At this point, mature adipocytes were largely derived from adipose-derived stem/stromal cells of grafts. Although vascular wall constituents were chiefly graft derived, vascular endothelial cells originated equally from graft and host bone marrow. Adipose-derived stem/stromal cells of regenerated fat were an admixture of grafted, host nonbone marrow, and host bone marrow cells.

Conclusions: The above findings underscore the importance of adipose stem/stromal cells in the grafted fat for adipocyte regeneration. Host bone marrow and local tissues contributed substantially to capillary networks and provided new adipose-derived stem/stromal cells. An appreciation of mechanisms that are operant in this setting stands to improve clinical outcomes of fat grafting and cell-based therapies. (*Plast. Reconstr. Surg.* 135: 00, 2015.)

Fat grafting has been increasingly recognized for its many clinical benefits, aside from tissue volumization. Tissues depleted of stem cells may be corrected by stem cell–containing tissue grafts. Grafted fat has the potential to revitalize diseased tissues (irradiated, dystrophic, or ischemic) and painful scars, thanks to contributing adipose-derived stem/stromal cells and tissue. However, such benefits are achieved only when each procedural step of fat grafting is properly executed. Hence, it seems that there remains much room for technical improvement.

From the Departments of Plastic Surgery and Cardiology, University of Tokyo Graduate School of Medicine.
Received for publication September 17, 2014; accepted December 29, 2014.

DOI: 10.1097/PRS.0000000000001292

Adipose tissue harbors a variety of cells, namely adipocytes, adipose-derived stem/stromal cells, and blood vascular cells (endothelial and mural).[1] Isolated or cultured adipose-derived stem/stromal cells hold great therapeutic promise through their capacity for multilineage differentiation, paracrine activity, and immunomodulation.[2–6]

Disclosure: *The authors have no financial interest to declare in relation to the content of this article.*

Supplemental digital content is available for this article. Direct URL citations appear in the text; simply type the URL address into any Web browser to access this content. Clickable links to the material are provided in the HTML text of this article on the *Journal*'s Web site (www.PRSJournal.com).

Consequently, clinical investigations of adipose-derived stem/stromal cells are aimed at a multiplicity of disorders[7,8]

Adipose-derived stem/stromal cells are heavily involved in the remodeling of adipose tissue after trauma of any nature, including ischemia-reperfusion injury, mechanical force, and grafting.[9–12] Through previous efforts, we have delineated a range of events that occur during remodeling, particularly the replacement of adipocytes by next-generation cells after fat is grafted.[12,13] Although cells such as adipose-derived stem/stromal cells, vascular endothelial cells, and macrophages are known participants in remodeling,[13,14] the origins of these constituents are unclear. It is acknowledged that adipose-derived stem/stromal cells facilitate mobilization and homing of bone marrow cells (such as endothelial progenitor cells)[15]; therefore, bone marrow–derived cells are likely components of regenerating fat after grafting.

In this study, we sought to investigate the origin of cells in the grafted fat after tissue remodeling/regeneration. We removed fat from green fluorescent protein (GFP) and wild-type mice for cross-transplantation (i.e., fat exchange) to investigate the origins of regenerating cells thereafter. In addition, mice with GFP–positive bone marrow served as recipients to research the fate of bone marrow–derived cells. We believe that a better appreciation of mechanisms inherent in the remodeling of grafted fat will improve related clinical outcomes and broaden the potential of stem cell therapies.

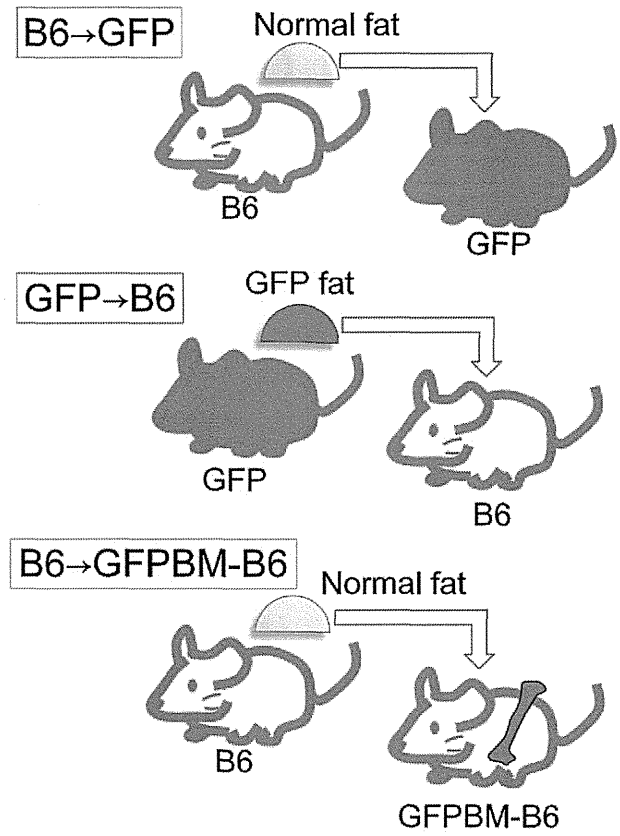

Fig. 1. Schematic diagram of experimental animal models. The inguinal fat pads of B6 mice were transplanted to GFP mice (B6→GFP), and those of GFP mice were transplanted to B6 mice (GFP→B6). GFP-positive bone marrow chimeric B6 mice (*GFPBM-B6*) were prepared by transplanting bone marrow of GFP mice into irradiated B6 mice. The fat pads of B6 mice were also transplanted to GFPBM-B6 mice (B6→GFPBM-B6).

MATERIALS AND METHODS

Animal Models

All animals were obtained from Japan SLC (Shizuoka, Japan; http://www.jslc.co.jp). Animal maintenance and experimental protocols were conducted under University of Tokyo guidelines.

Fat Exchange Models

Female 9-week-old mice of two strains, C57BL/6 (B6 mice) and C57BL/6-Tg (CAG-EGFP) (GFP mice), were anesthetized using intraperitoneal pentobarbital 50 mg/kg, and inguinal fat pads were harvested for cross-transplantation into subcutis of scalp, as described previously.[12] Fat pads of B6 mice were transplanted to GFP mice (B6→GFP), and fat pads of GFP mice were transplanted to B6 mice (GFP→B6) (Fig. 1). B6 and GFP mice are near-identical strains, so immune reactivity is negligible. At 1, 2, 4, and 12 weeks after transplantation, total body weight was recorded, and the grafted fat was harvested for further analyses, such as histology and flow cytometry. Thus, different animals were analyzed at each time point. Three animals for each group at each time point were analyzed for weight, histology, and stromal vascular fraction culture. Furthermore, nine animals for each group at 12 weeks were analyzed for fluorescence-activated cell sorting analysis of stromal vascular fraction. Bodily weight increases over time were similar in both grafted models. Graft weights were normalized (i.e., divided by body weights) to counter the effects of animal growth.

Bone Marrow Transplantation Model

GFP-positive bone marrow chimeric B6 mice (GFPBM-B6) were generated as reported previously.[16] Briefly, femoral and tibial bone marrow cells were harvested from 6-week-old female GFP mice by flushing with phosphate-buffered saline. After hemolysis with red blood cell lysis buffer (Sigma Aldrich, St. Louis, Mo.) and washing,

unfractionated GFP-positive bone marrow cells (2×10^6 cells/mice) were injected intravenously via tail veins into 6-week-old female B6 mice after lethal doses (10 Gy) of whole-body γ-irradiation. At week 6 after bone marrow transplantation, viable GFP-positive bone marrow chimeric cells were confirmed by flow cytometry of peripheral blood. Only mice with greater than 90 percent GFP-positive white blood cells (CD45-positive cells) were used for further study. After bone marrow transplantation (week 8), inguinal fat pads of B6 mice were transplanted beneath scalps of GFPBM-B6 mice (B6→GFPBM-B6) (Fig. 1). Transplanted fat was then harvested 12 weeks after grafting.

Immunohistochemistry

Graft samples were fixed (Zinc Fixative; BD Biosciences, San Jose, Calif.), embedded in paraffin, and sectioned at 6 μm. The following primary antibodies were used: rabbit anti-GFP (Novus Biologicals, Littleton, Colo.), guinea pig anti-perilipin (Progen, Heidelberg, Germany), and rat anti-MAC-2 (Cedarlane Laboratories, Burlington, Ontario, Canada). Isotypic antibodies served as negative controls for each marker. Secondary antibodies (anti-rabbit Alexa Fluor 488 or anti-guinea pig Alexa Fluor 568) were applied as appropriate. Nuclei and vascular endothelial cells were delineated by Hoechst 33342 (Dojindo, Tokyo, Japan) and Alexa Fluor 647–conjugated lectin (Life Technologies Corp., Carlsbad, Calif.), respectively. Sections were examined via fluorescence (Keyence, Osaka, Japan) or confocal (TCS SP2 system; Leica, Heerbrugg, Switzerland) microscopy.

Whole-Mount Staining

Staining of fresh whole-mount tissue samples was also carried out, as described previously.[9] Briefly, 3-mm sections of adipose tissue were incubated for 30 minutes at 37°C with Alexa Fluor 568–conjugated or 647-conjugated lectin (Life Technologies), targeting vascular endothelial cells, and Hoechst 33342 (Dojindo), directed at nuclei. GFP was detectable without staining. Washed samples were examined via confocal microscopy (Leica TCS SP2 system). Serial images were recorded at 1-μm intervals, producing surface-rendered three-dimensional images.

Stromal Vascular Fraction Isolation

Adipose tissue was minced into 1-mm pieces and digested in phosphate-buffered saline plus 0.075 percent collagenase (Wako Pure Chemical Industries, Ltd., Osaka, Japan) for 30 minutes on a shaker at 37°C. Solutes were then washed, filtered (100-μm and 30-μm mesh), and centrifuged (800 *g* for 5 minutes). Erythrocytes were extracted using lysis buffer (Sigma Aldrich).

Portions of stromal vascular fraction cells were cultured in M199 medium (GIBCO Invitrogen, Carlsbad, Calif.) containing 10% fetal bovine serum, 100 IU of penicillin, 100 mg/ml streptomycin, 5 μg/ml heparin, and 2 ng/ml fibroblast growth factor-1. Contaminants, such as leukocytes and vascular endothelial cells, disappeared after passaging, and only adipose-derived stem/stromal cells were selectively expanded.[17] Adipose-derived stem/stromal cells at second passage were examined under fluorescence microscopy (Keyence) to ascertain GFP-positive cells.

Flow Cytometry Analysis

Stromal vascular fraction cells were identified by surface marker expression via flow cytometry, harvesting stromal vascular fraction cells of three mice for each experiment; analyses were performed in triplicate. Cells were incubated with rat anti-CD34-biotin antibodies (eBioscience, San Diego, Calif.) at 4°C for 30 min. After a wash with phosphate-buffered saline, the following secondary antibody and monoclonal antibody–fluorescein conjugates were applied at 4°C for 30 min: rat anti-streptoavidin-allophycocyanin, rat anti-CD31-fluorescein phycoerythrin (BD Bioscience), and rat anti-CD45-phycoerythrin Cy7 (eBioscience). GFP was detectable without staining. Cells were then analyzed using an LSR II flow cytometry system (BD Biosciences). Adipose-derived stem/stromal cells and vascular endothelial cells were determined as $D45^-/CD34^+/CD31^-$ cells and $CD45^-/CD34^+/CD31^+$ cells, respectively. Inguinal fat pads of normal GFP and B6 mice were also monitored as controls.

There were 4.6 ± 1.9 percent false-positives in B6 mice and 24.0 ± 1.1 percent false negatives in GFP mice (**see Figure, Supplemental Digital Content 1**, which shows a representative flow cytometric analysis of six varied samples. Adipose-derived stem/stromal cells and vascular endothelial cells were determined as $CD45^-/CD34^+/CD31^-$ cells and $CD45^-/CD34^+/CD31^+$ cells, respectively, ***http://links.lww.com/PRS/B296***). Data initially recorded were corrected as follows: *Corrected proportion* [percent] = 100 × (*Naïve data percent – GFP percent of B6 mice*) / (*GFP percent of GFP mice – GFP percent of B6 mice*).

Statistical Analysis

Results are expressed as median (quartile 1 to quartile 3). The Mann-Whitney test was used for

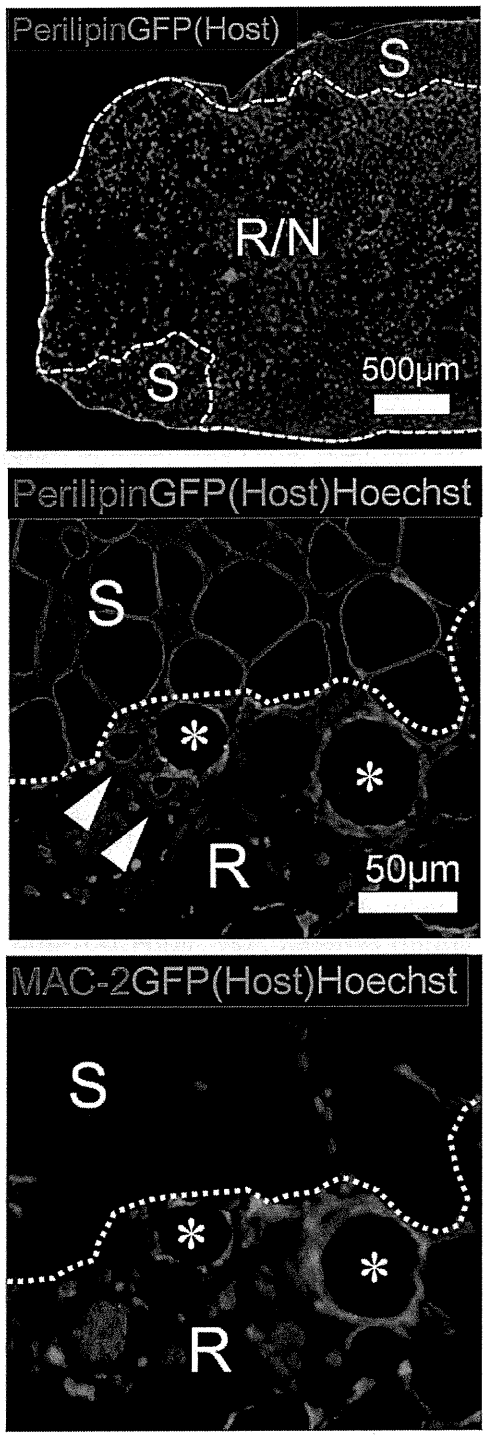

Fig. 2. Adipocyte degeneration/regeneration and host-cell infiltration. Immunostained sequential sections of inguinal fat at 1 week after transplantation are shown. (*Above*) The yellow interrupted line marks the border of surviving (*S*; perilipin-positive) and regenerating/necrotizing (*R/N*; perilipin-negative) tissue. Adipocytes undergo zonal necrosis resulting from ischemia, whereas superficial cells remain viable through plasmatic diffusion from peripheral host tissue. Infiltrating host cells (GFP-positive) predominate in regenerating areas. *Bar* = 500 μm. Sections of B6→GFP model stained for perilipin (adipocyte marker; *center*) and MAC-2 (macrophage marker; *below*) with Hoechst stain and GFP, respectively. Surviving (*S*) and regenerating (*R*) zones of adipocytes are clearly demarcated by perilipin staining (*dotted line*). Host cells infiltrated regenerating areas only and were mostly MAC-2-positive macrophages. The *asterisk* indicates crown-like structure (necrotic adipocytes rimmed by phagocytic macrophages). *Arrowheads* highlight graft-derived (GFP-negative) regenerating adipocytes. *Bars* = 50 μm. (*Below*) MAC-2-positive cells quantified relative to all host cells. Nonmacrophage host cells (MAC-2$^-$/GFP$^+$) rose in number over time. Data are expressed as median (quartile 1 to quartile 3).

two-group comparisons. Bonferroni correction was used for multiple testing. Statistical significance was otherwise set at $p < 0.05$.

RESULTS

Tissue Regeneration/Remodeling after Fat Grafting

In both exchange models (B6→GFP and GFP→B6), normalized weights of inguinal fat grafts reduced over time since 2 weeks after grafting and was approximately one-half of control at 12 weeks. The graft weight of respective models did not differ statistically at either time point. [**See Figure, Supplemental Digital Content 2,** which shows sequential changes in normalized graft weight of both fat exchange models. Weights of graft samples were normalized, dividing sample weight by body weight. Normalized weight ratios did not differ significantly by graft model (B6→GFP versus GFP→B6). Data are expressed as median (quartile 1 to quartile 3), ***http://links.lww.com/PRS/B297.***]

Grafted adipose tissue underwent total tissue remodeling, as we reported previously.[12,13] Immunohistochemistry of B6→GFP and GFP→B6 models revealed localization of host-derived and graft-derived cells (GFP-positive cells), respectively. With the exception of the most superficial perilipin-positive survival zone (100 to 500 μm from graft surface), all adipocytes were necrotic (perilipin-negative) by 1 week (Fig. 2, *above*). F2
Perilipin is a protein that coats lipid droplets in adipocytes and is detectable only in viable adipocytes.[12] Regenerating and necrotizing zones were then partly replaced by resident and infiltrating stem/progenitor cells. The adipocyte regeneration was complete by 12 weeks.

At 1 week, numerous host cells infiltrated in regenerating/necrotizing perilipin-negative zones but not the viable perilipin-positive survival zone (Fig. 2, *center*). Sequential sections showed that infiltrating host cells were primarily

MAC-2–positive macrophages, and crown-like structures (necrotic adipocytes rimmed by macrophages) were noted (Fig. 2, *below*). Small (<30 μm), regenerative, perilipin-positive adipocytes were also observed at the peripheries of regenerating zones. Temporal quantification of cell types confirmed that host cells were mainly MAC-2–positive macrophages (Fig. 3), which peaked at F3 2 weeks (>90 percent) and later declined [62.6 percent (range, 56.3 to 69.9 percent) at 12 weeks; $n = 3$]. At completion of regeneration (12 weeks), scavenging of oil drops was still in progress.

Immunohistologic Assessment of Regenerated Adipocytes

Origins of cells in regenerated adipose tissue were assessed in grafted samples at 12 weeks, with a focus on adipocytes, vessel wall structures, capillaries (vascular endothelial cells), and adipose-derived stem/stromal cells.

In sections of the B6→GFP model, perilipin-negative areas (oil drops) were surrounded by GFP-positive macrophages. However, regenerating perilipin-positive adipocytes barely expressed GFP, suggesting that most of the adipocytes were F4 of graft origin (Fig. 4, *above*). This was corroborated by sections of the GFP→B6 model, in which nearly all perilipin-positive adipocytes expressed GFP (the graft marker here) (Fig. 4, *below*). Furthermore, host-derived adipocytes (GFP-positive/perilipin-negative cells in the B6→GFP model; GFP-negative/perilipin-positive cells in the GFP→B6 model) were exceedingly rare (Fig. 4, *below*), and GFP-positive adipocytes were undetectable in the B6→GFPBM-B6 model. Thus, nearly all regenerated adipocytes were derived from adipocyte progenitors (adipose-derived stem/stromal cells) in grafted tissue, with negligible host-derived contributions.

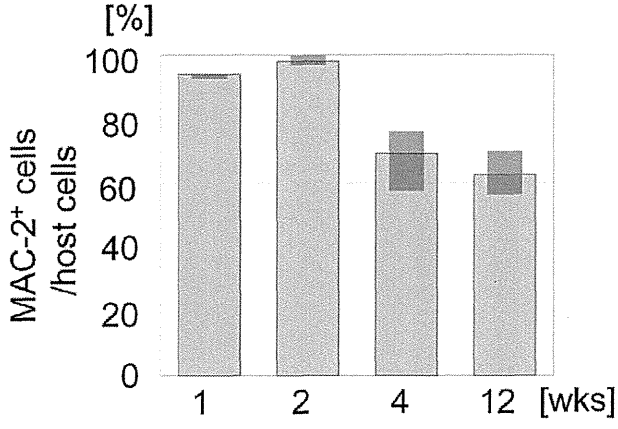

AQ6 **Fig. 3.** MAC-2-positive cells quantified relative to all host cells. Nonmacrophage host cells (MAC-2⁻/GFP⁺) rose in number over time. Data are expressed as median (quartile 1 to quartile 3).

Immunohistologic Assessment of Vessel Wall Cells and Capillaries

Large vessels were identified morphologically under phase contrast imaging, and vascular wall smooth muscle cells were evaluated via immunohistochemistry. Host-derived cells accounted for 15.4 percent (range, 11.7 to 17.5 percent) in B6→GFP samplings ($n = 9$) and 36.0 percent (range, 26.1 to 41.8 percent) in GFP→B6 samplings ($n = 9$), indicating a predominance of graft-derived cells (Fig. 5). F5

Stained whole-mount samples clearly showed that graft-derived and host-derived cells were equally represented in chimeric capillaries of both B6→GFP and GFP→B6 models (Fig. 6, *above* and F6 *center*). This was confirmed by immunostained sections. To further investigate the contribution of host bone marrow–derived cells, whole-mount samples of the B6→GFPBM-B6 model were also stained. Chimeric capillaries, formed through contributing host bone marrow–derived cells (Fig. 6, *below*), were similarly seen.

Flow Cytometric Analysis of Stromal Vascular Fraction

GFP-positive cells were quantified by flow cytometry of stromal vascular fraction cells (i.e., fat constituents other than adipocytes), isolated through collagenase digestion of graft samples. Adipose-derived stem/stromal cells and vascular endothelial cells were identified as $CD45^-/CD34^+/CD31^-$ cells and $CD45^-/CD34^+/CD31^+$ cells, respectively. Representative data of six samples (B6, GFP, B6→GFP, GFP→B6, GFPBM-B6, and B6→GFPBM-B6) are shown in Figure 7 (*above*) F7 and in **Figure, Supplemental Digital Content 1**, ***http://links.lww.com/PRS/B296***. Initial flow cytometry data were corrected as described (see Materials and Methods), and resultant data on cellular origins are shown in Figure 7 (*center*). Our findings suggest that adipose-derived stem/stromal cells were both graft-derived and host-derived, and that host-derived adipose-derived stem/stromal cells were similarly of bone marrow and non–bone marrow derivation. Therefore, surrounding recipient tissue likely supplied some adipose-derived stem/stromal cells during the process of regeneration. Vascular endothelial cells were also composed of graft and host cells to a similar extent, but the host contribution was mostly from bone marrow, with a negligible non–bone marrow component.

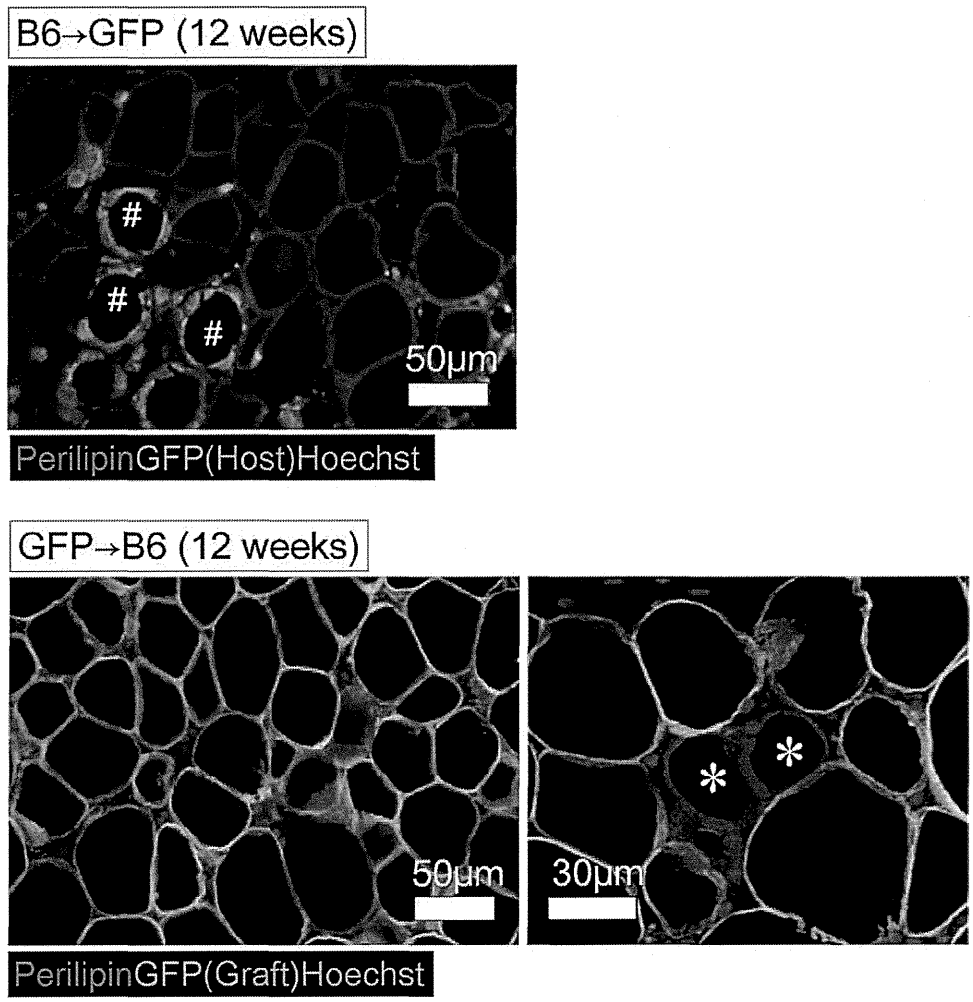

Fig. 4. Origin of regenerated mature adipocytes in exchanged fat. (*Above*) In the B6→GFP model, most mature adipocytes (perilipin-positive) at 12 weeks are GFP-negative (graft-derived). GFP-positive cells surrounding oil drops (#) are chiefly macrophages. *Bars* = 30 μm. (*Below*) In the GFP→B6 model, most mature adipocytes (perilipin-positive) at 12 weeks are GFP-positive (graft-derived) and thus appear yellow (*left*). Host-derived adipocytes (perilipin-positive/GFP-negative) (*) are very rarely detected (*right*). *Bar* = 50 μm (*left*) and 30 μm (*right*).

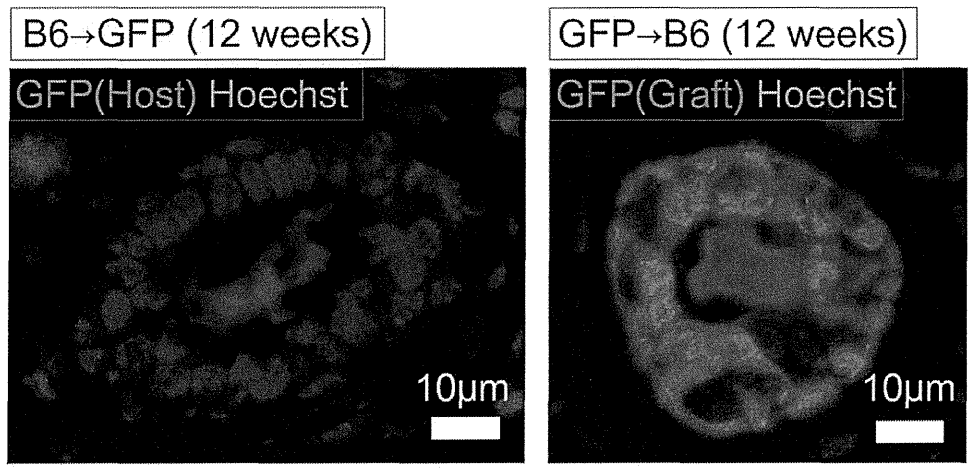

AQ7

Fig. 5. Origin of vessels and capillaries in exchanged fat tissue. Large vessels chiefly incorporated graft-derived smooth muscle cells in both B6→GFP (*left*) and GFP→B6 (*right*) models. *Bar* = 10 μm.

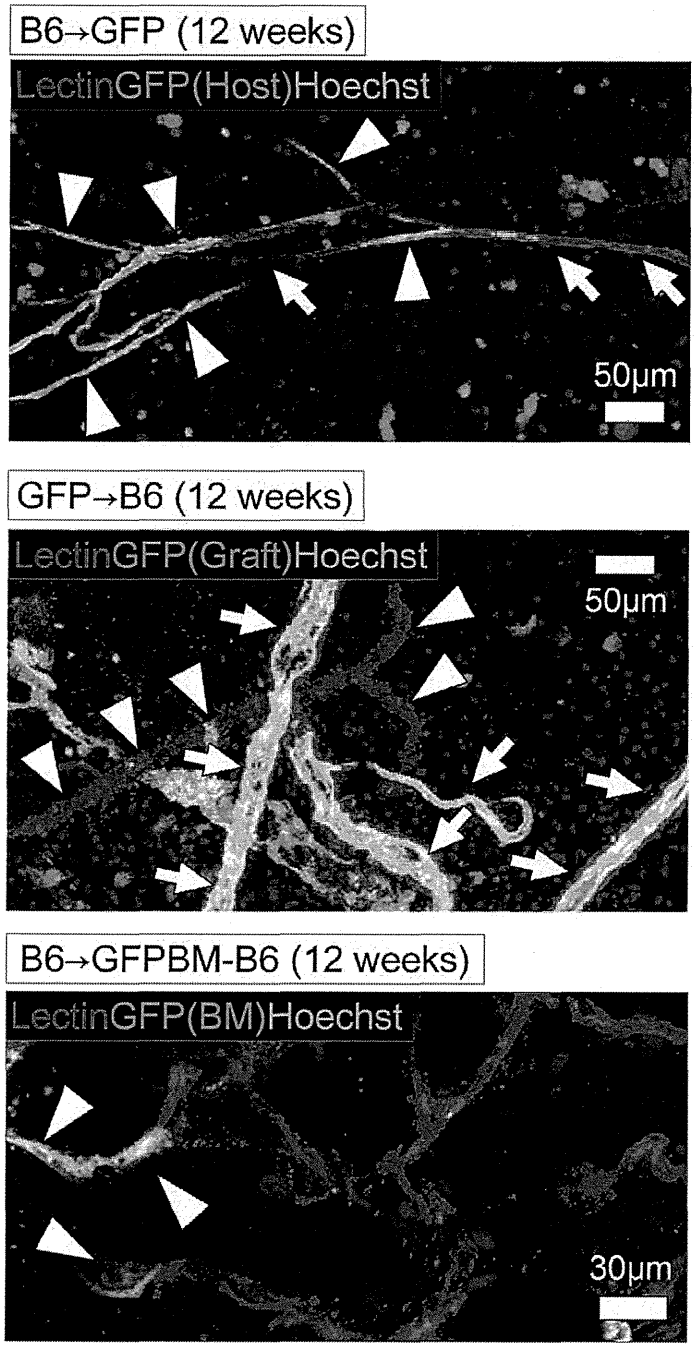

Fig. 6. Origin of vessels and capillaries in exchanged fat tissue. Stained whole-mount samples of B6→GFP (*above*) and GFP→B6 (*center*) models show graft/host chimeric capillaries. *Arrows* indicate graft-derived vascular endothelial (lectin-positive) cells; *arrowheads* highlight host-derived endothelial cells. *Bar* = 50 μm. (*Below*) Stained whole-mount samples of the B6→GFPBM-B6 model showing lectin-positive/GFP-positive host bone marrow–derived vascular endothelial cells. *Bar* = 30 μm.

Stromal vascular fraction cells from B6→GFP and GFP→B6 samples were cultured (Fig. 7, *below, left*). Flow cytometric data of cultured adipose-derived stem/stromal cells were comparable to those of noncultured adipose-derived stem/stromal cells (Fig. 7, *below, right*). Host proportions were 67.7 percent (range, 62.7 to 80.0 percent $n = 3$) and 49.2 percent (range, 33.3 to 67.7 percent; $n = 3$)

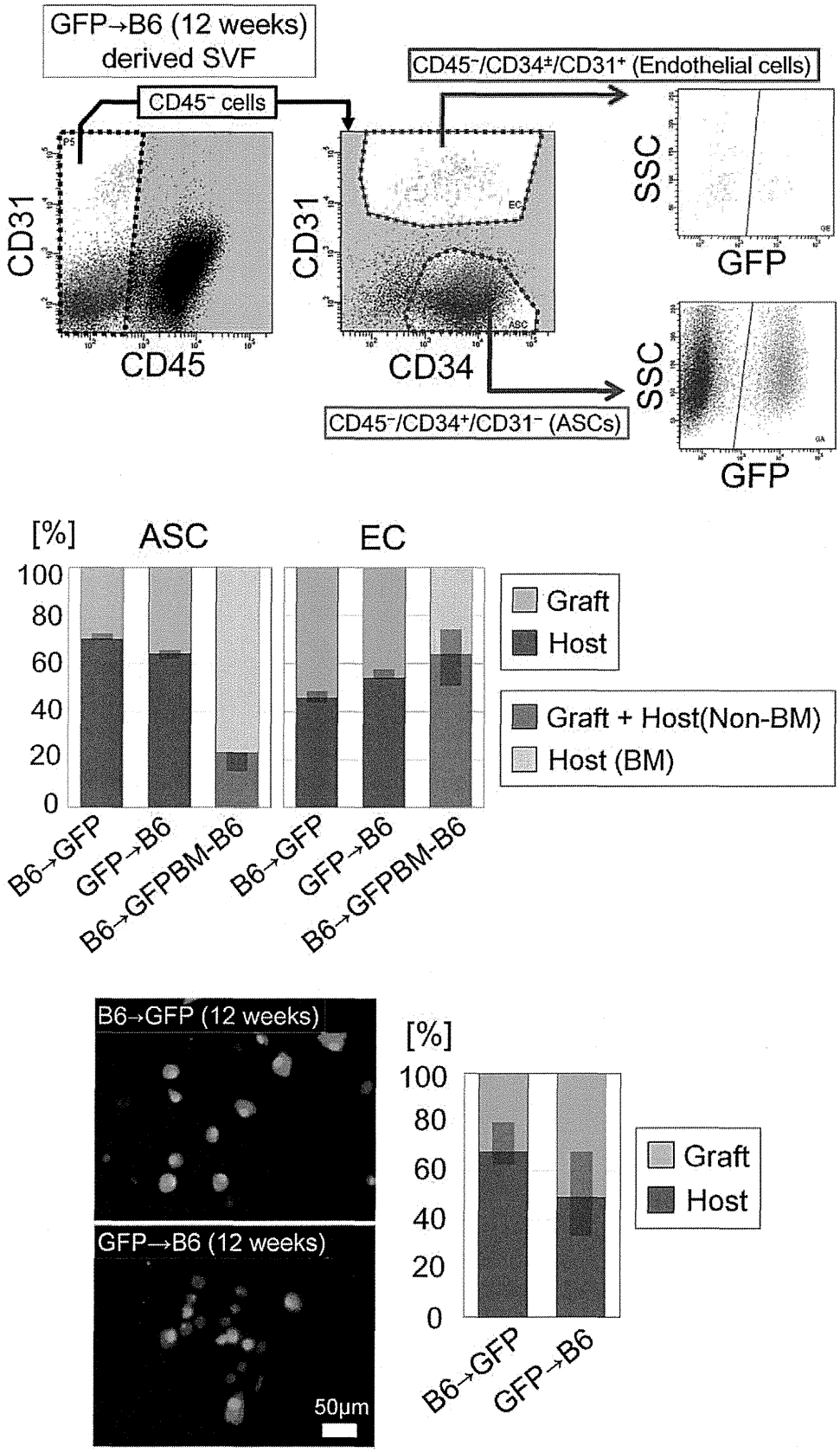

Fig. 7. Analysis of stromal vascular fraction cells isolated from exchanged fat. Freshly isolated or cultured stromal vascular fraction cells from fat samples (three each) of B6→GFP and GFP→B6 models analyzed at 12 weeks. Adipose-derived stem/stromal cells (*ASCs*) and vascular endothelial cells (*ECs*) were determined by flow cytometry ($CD45^-/CD34^+/CD31^-$ cells

in adipose-derived stem/stromal cells of B6→GFP and GFP→B6 models, respectively.

DISCUSSION

Our previous studies[12,13] suggested that adipose tissue is remodeled during the first 3 months, but the cellular origin of regenerated adipose tissue remained unknown. Using the histological and flow cytometrical data of this study, we summarized the origin of each cellular component in grafted/regenerated fat tissue in Table 1. Except for surviving adipocytes that were superficially located, all other adipocytes are supposed to be regenerated mostly from graft-resident adipose-derived stem/stromal cells. Most of the vascular mural cells are also derived from the graft, whereas nearly half of vascular endothelial cells originate from bone marrow of the host. Adipose-derived stem/stromal cells were a mixture of the graft, the host nonbone marrow, and the host bone marrow. The discrepancy in cellular origin between adipocytes and adipose-derived stem/stromal cells suggested that adipose-derived stem/stromal cells have to reside next to adipocytes to become adipocytes upon adipocyte death, although new adipocytes can be provided from surrounding tissue and bone marrow.

Tissue remodeling in grafted fat was initiated by zonal adipocyte necrosis, triggering adipose-derived stem/stromal cell activation and host cell infiltration by 1 week. Host-cell infiltrates at the early inflammatory phase of repair were almost exclusively macrophages, although by week 12 their percentage had declined to 60 percent, suggesting that other types of cells were involved in later phases of regeneration. Previously, we alluded to the differential roles of inflammatory (M1) macrophages and anti-inflammatory (M2) macrophages in the remodeling of fat.[13,14] M1 macrophages surround and phagocytize necrotic adipocytes (lipid droplets), whereas M2 macrophages appear to take part in scar/capsule formation.

Table 1. Origins of Cellular Components in Grafted Fat

		Host	
	Graft	Non–Bone Marrow	Bone Marrow
Adipocytes	++++	±	–
Vascular mural cells	+++	+	±
Vascular endothelial cells	++	±	++
Adipose-derived stem/stromal cells	++	++	++

Herein, the origins of cellular elements in grafted fat were evaluated at 12 weeks, which reportedly is the time interval required to complete the regeneration of grafts. However, phagocytosis and scar formation are still ongoing beyond this point. Outcomes of our fat exchange graft models clearly indicate the differential contribution of graft-derived and host-derived cells in regenerating/remodeling adipose tissue. New host-derived adipocytes (likely contributed by migrating adipose-derived stem/stromal cells of peripheral host tissue) were rarely detected. Instead, nearly all adipocytes originated from grafts alone. On the other hand (and interestingly), adipose-derived stem/stromal cells found in regenerated fat as future contributors to adipose remodeling were of graft and host origins. Flow cytometric analysis and our experimental bone marrow transplantation in mice suggested that not all host-derived adipose-derived stem/stromal cells originate from bone marrow. A substantial number of stem/progenitor cells likely migrated into grafts from local host tissue as well resided as adipose-derived stem/stromal cells in regenerated fat. Indeed, a previous report has shown that adipose tissue may even release adipose-derived stem/stromal cells into lymphatic flow, and this mobilization of adipose-derived stem/stromal cells may be controlled by CXCR4.[18]

The discrepancy between observed origins of adipocytes and adipose-derived stem/stromal cells is unexplained as yet. Some studies have suggested that bone marrow–derived cells (M2 macrophages) home to adipose tissue and may transform into adipose-derived stem/stromal cells,[19–21] and bone marrow-derived cells are capable of adipocyte differentiation under non-physiologic experimental conditions, such as a chamber neogenesis model.[22,23] Still, adipocytes

Fig. 7. (*Continued*) and $CD45^-/CD34^+/CD31^+$ cells, respectively). (*Above*) Representative flow cytometric data of stromal vascular fraction cells isolated from GFP→B6 sample at 12 weeks are shown. *SSC*, side scatter. (*Center*) Origins of adipose-derived stem/stromal cells and vascular endothelial cells in samples of B6→GFP, GFP→B6, and B6→GFPBM-B6 models. Flow cytometry confirmed that both adipose-derived stem/stromal cells and vascular endothelial cells were mixtures of graft-derived and host-derived cells. Host-contributed adipose-derived stem/stromal cells were both non–bone marrow– and bone marrow–derived, whereas host-contributed vascular endothelial cells were primarily bone marrow derivatives. Data are expressed as median (quartile 1 to quartile 3) ($n = 3$ at each time point). (*Below, left*) Cultured adipose-derived stem/stromal cells from samples of B6→GFP and GFP→B6 models under fluorescent microscope. (*Below, right*) Graft/host ratio of cultured adipose-derived stem/stromal cells. Data are expressed as median (quartile 1–quatile 3).

derived from bone marrow are rarely found in mice on normal or high-fat diets.[16,19] Nevertheless, our findings plainly indicate that adipose-derived stem/stromal cells in the grafted tissue are crucial for adipocyte regeneration after fat grafting.

In addition, we found that mural cells (vascular smooth muscle cells) were largely of graft derivation, whereas the origins of vascular endothelial cells were quite different. Both histologic and flow cytometric analyses revealed a mix of graft and host origins for these cells. Unlike adipose-derived stem/stromal cells, our experimental transplantation of mouse bone marrow suggested that nearly all host-derived vascular endothelial cells originate from bone marrow. This means that a substantial number of endothelial progenitor cells are mobilized from bone marrow, resulting in a capillary network chimera. Similar graft/host chimeric capillaries have been observed after kidney transplantation.[24] Hence, capillary remodeling in the aftermath of fat grafting technically is a culmination of vasculogenesis, rather than angiogenesis.

CONCLUSIONS

The clinical implications of this study are considerable in terms of homeostasis/remodeling in adipose tissue and repair/regeneration of grafted fat. Next-generation adipocytes in fat grafts are derived from adipose-derived stem/stromal cells in the graft, but new adipose-derived stem/stromal cells for future remodeling are also provided by bone marrow and other local (adipose) tissue elements. Adipose tissue may also serve as a reservoir of adipose-derived stem/stromal cells from circulation. Although graft-derived vascular structures are involved in revascularization after fat grafting, endothelial progenitor cells mobilized from bone marrow are major contributors as well. We believe that understanding the mechanisms of fat grafting would strategically improve current grafting procedures. Our findings also propose future studies that explore novel methods to manipulate activation, migration, or homing of graft-derived and bone marrow–derived stem/progenitor cells.

Kotaro Yoshimura, M.D.
Department of Plastic Surgery
University of Tokyo School of Medicine
7-3-1, Hongo, Bunkyo-Ku
Tokyo 113-8655, Japan
kotaro-yoshimura@umin.ac.jp

ACKNOWLEDGMENTS

This study was supported by the Japanese Ministry of Education, Culture, Sports, Science, and Technology (Grant-in-Aid for Scientific Research B3-24390398). The authors greatly appreciate the substantial contributions to this study by Drs. Kazuhide Mineda and Takanobu Mashiko. They also thank Ayako Sato for technical assistance.

REFERENCES

1. Eto H, Suga H, Matsumoto D, et al. Characterization of structure and cellular components of aspirated and excised adipose tissue. *Plast Reconstr Surg.* 2009;124:1087–1097.
2. Safford KM, Hicok KC, Safford SD, et al. Neurogenic differentiation of murine and human adipose-derived stromal cells. *Biochem Biophys Res Commun.* 2002;294:371–379.
3. Tholpady SS, Katz AJ, Ogle RC. Mesenchymal stem cells from rat visceral fat exhibit multipotential differentiation in vitro. *Anat Rec A Discov Mol Cell Evol Biol.* 2003;272:398–402.
4. Safford KM, Safford SD, Gimble JM, et al. Characterization of neuronal/glial differentiation of murine adipose-derived adult stromal cells. *Exp Neurol.* 2004;187:319–328.
5. Seo MJ, Suh SY, Bae YC, Jung JS. Differentiation of human adipose stromal cells into hepatic lineage in vitro and in vivo. *Biochem Biophys Res Commun.* 2005;328:258–264.
6. Yanez R, Lamana ML, Garcia-Castro J, et al. Adipose tissue-derived mesenchymal stem cells have in vivo immunosuppressive properties applicable for the control of the graft-versus-host disease. *Stem Cells* 2006;24:2582–2591.
7. Casteilla L, Planat-Benard V, Laharrague P, et al. Adipose-derived stromal cells: Their identity and uses in clinical trials, an update. *World J Stem Cells.* 2011;3:25–33.
8. Gimble JM, Guilak F, Bunnell BA. Clinical and preclinical translation of cell-based therapies using adipose tissue-derived cells. *Stem Cell Res Ther.* 2010;1:19. AQ9
9. Suga H, Eto H, Shigeura T, et al. IFATS collection: Fibroblast growth factor-2-induced hepatocyte growth factor secretion by adipose-derived stromal cells inhibits postinjury fibrogenesis through a c-Jun N-terminal kinase-dependent mechanism. *Stem Cells* 2009;27:238–249.
10. Kato H, Suga H, Eto H, et al. Reversible adipose tissue enlargement induced by external tissue suspension: Possible contribution of basic fibroblast growth factor in the preservation of enlarged tissue. *Tissue Eng Part A* 2010;16:2029–2040.
11. Suga H, Eto H, Aoi N, et al. Adipose tissue remodeling under ischemia: Death of adipocytes and activation of stem/progenitor cells. *Plast Reconstr Surg.* 2010;126:1911–1923.
12. Eto H, Kato H, Suga H, et al. The fate of adipocytes after nonvascularized fat grafting: Evidence of early death and replacement of adipocytes. *Plast Reconstr Surg.* 2012;129:1081–1092.
13. Kato H, Mineda K, Eto H, et al. Degeneration, regeneration, and cicatrization after fat grafting: Dynamic total tissue remodeling during the first 3 months. *Plast Reconstr Surg.* 2014;133:303e–313e.
14. Mineda K, Kuno S, Kato H, et al. Chronic inflammation and progressive calcification as a result of fat necrosis: The worst end in fat grafting. *Plast Reconstr Surg.* 2014;133:1064–1072.
15. Dimarino AM, Caplan AI, Bonfield TL. Mesenchymal stem cells in tissue repair. *Front Immunol.* 2013;4:201. AQ10
16. Tomiyama K, Murase N, Stolz DB, et al. Characterization of transplanted green fluorescent protein+ bone marrow cells into adipose tissue. *Stem Cells* 2008;26:330–338.
17. Yoshimura K, Shigeura T, Matsumoto D, et al. Characterization of freshly isolated and cultured cells derived from the fatty and fluid portions of liposuction aspirates. *J Cell Physiol.* 2006;208:64–76.

18. Gil-Ortega M, Garidou L, Barreau C, et al. Native adipose stromal cells egress from adipose tissue in vivo: Evidence during lymph node activation. *Stem Cells* 2013;31:1309–1320.
19. Crossno JT Jr, Majka SM, Grazia T, et al. Rosiglitazone promotes development of a novel adipocyte population from bone marrow-derived circulating progenitor cells. *J Clin Invest.* 2006;116:3220–3228.
20. Hausman GJ, Hausman DB. Search for the preadipocyte progenitor cell. *J Clin Invest.* 2006;116:3103–3106.
21. Eto H, Ishimine H, Kinoshita K, et al. Characterization of human adipose tissue-resident hematopoietic cell populations reveals a novel macrophage subpopulation with CD34 expression and mesenchymal multipotency. *Stem Cells Dev.* 2013;22:985–997.
22. Stillaert F, Findlay M, Palmer J, et al. Host rather than graft origin of Matrigel-induced adipose tissue in the murine tissue-engineering chamber. *Tissue Eng.* 2007;13:2291–2300.
23. Lee YH, Petkova AP, Granneman JG. Identification of an adipogenic niche for adipose tissue remodeling and restoration. *Cell Metab.* 2013;18:355–367.
24. Lagaaij EL, Cramer-Knijnenburg GF, van Kemenade FJ, et al. Endothelial cell chimerism after renal transplantation and vascular rejection. *Lancet.* 2001;357:33–37.

AUTHOR QUERIES

AUTHOR PLEASE ANSWER ALL QUERIES

AQ1—Please provide the hightest degree earned for all authors.

AQ2—GFP spelled out correctly as "green fluorescent protein"? If not, please provide the correct expansion.

AQ3—It looks like ref 15 is meant here, rather than ref 18 as in original manuscript. Okay to cite ref 15 here? If not, please cite ref 15 in text where wanted, renumbering as needed so that refs are cited in numerical order, per Journal style.

AQ4—GFP defined correctly as "green fluorescent protein"? If not, please provide the correct definition.

AQ5—Please provide name and city/state location of manufacturer of Alexa Fluor secondary antibodies, per Journal style for use of brand names.

AQ6—Original Figure 2 was divided into Figures 2 and 3 by the editorial office, and subsequent figures were renumbered accordingly. Please confirm that figure legends are correct as divided/edited.

AQ7—Original Figure 4 was divided into Figures 5 and 6. Legends correct as edited? Please advise/revise as needed.

AQ8—Figure panels correct as described in the legend to Figure 7 (i.e., "Below, left" and "Below, right")? If not, please revise as needed.

AQ9—Please supply ending folio for ref 8, for a complete page range.

AQ10—Please supply ending folio for ref 15, for a complete page range.

AQ11—Please confirm that disclosure statement is correct as edited. Grant information has been moved to the Acknowledgments section, per Journal style.

4. Miteva M, de Farias DC, Zaiac M, Romanelli P, Tosti A. Nail clipping diagnosis of onychomatricoma. Arch Dermatol 2011;147:1117–8.

5. Perrin C, Langbien L, Schweizer J, Cannata G, et al. Onychomatricoma in the light of the microanatomy of the normal nail unit. Am J Dermatopath 2011;33:131–9.

Michael S. Graves, MD
J. Kelly Anderson, BS
Section of Dermatology
Medical College of Georgia
Georgia Regents University
Augusta, Georgia

Keith G. LeBlanc Jr, MD
The Skin Surgery Centre
Metairie, Louisiana

Daniel J. Sheehan, MD
Section of Dermatology
Medical College of Georgia
Georgia Regents University
Augusta, Georgia

The authors have indicated no significant interest with commercial supporters.

A Novel Facial Rejuvenation Treatment Using Pneumatic Injection of Non–Cross-Linked Hyaluronic Acid and Hypertonic Glucose Solution

Expectations for minimally invasive procedures have increased recently in the field of cosmetic surgery because of the large number of patients hoping to avoid invasive surgery. "Subdermal minimal surgery" technology, a computerized system that enables the targeted delivery of a jet of a solution by high pneumatic pressure through a tiny orifice, is a novel therapeutic modality for dermal remodeling procedures, such as those involving neck wrinkles, keloids, and depressed scars due to acne or herpes zoster.[1–4] In previous clinical studies, it was suggested that pneumatically injected hyaluronic acid (HA) particles promote wound healing and induce neocollagenesis.[1–4] The authors have applied this pneumatic technology to nonsurgical facial tightening, modifying the technology to suit the specific needs of this procedure.

Treatment Procedures

The injection system (Enerjet; PerfAction Ltd., Rehovot, Israel) consisted of a central console, applicator, and sterile disposable kit mounted on an applicator. The applicator was filled with a mixed solution of 1 mL non–cross-linked HA (Artz; Seikagaku Corporation, Tokyo, Japan) and 9 mL 20% glucose solution (Fuso Pharmaceutical Industries, Osaka, Japan), which were compounded using a sterile 3-way stopcock and 2 syringes. The authors expected that the

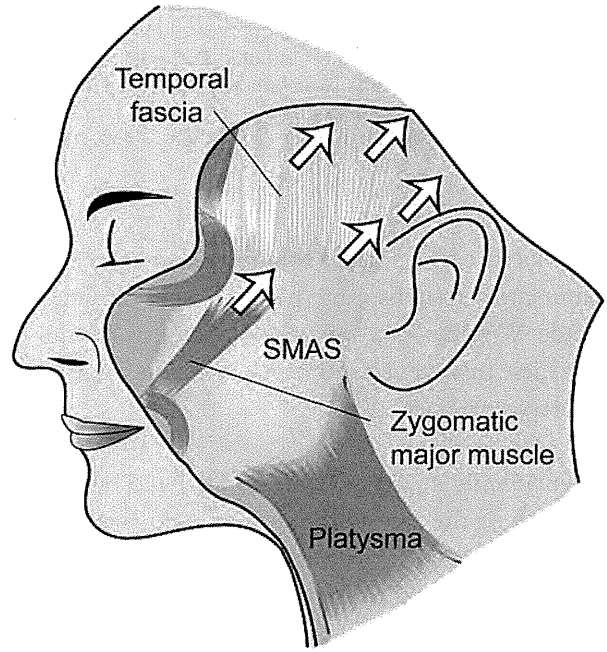

Figure 1. Placement of the pneumatic injections (white arrows). Temporal along the hairline, temporal within the main hair mass, supra-auricular, preauricular along the zygomatic arch, and malar prominence. SMAS, superficial musculoaponeurotic system.

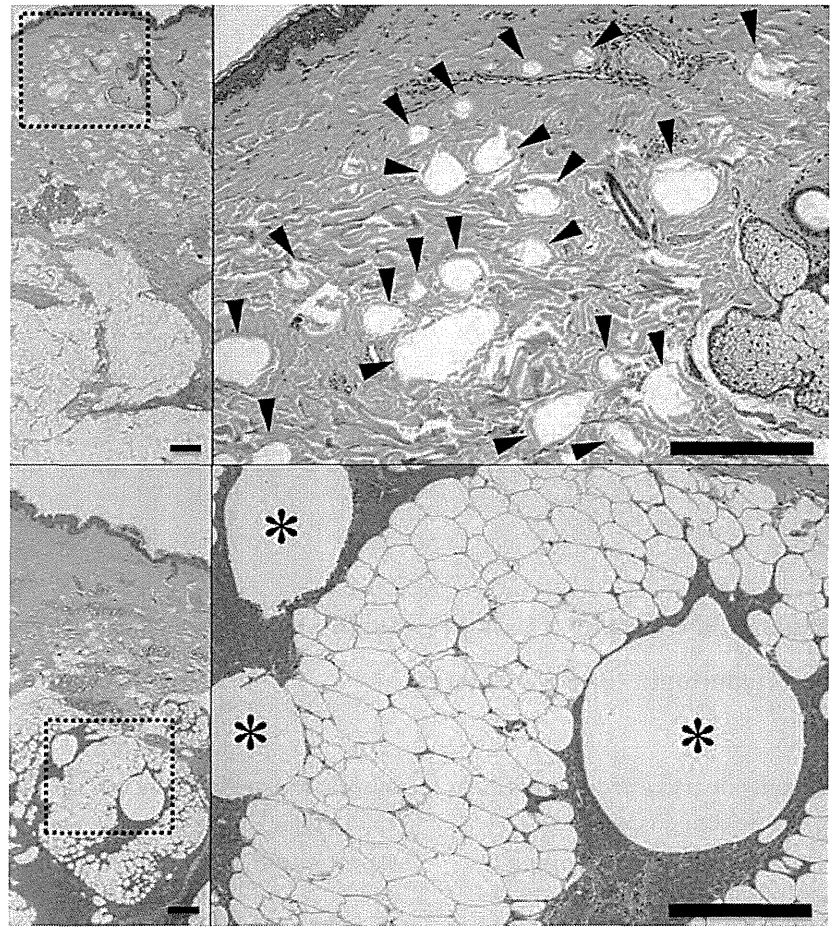

Figure 2. Histological analysis of the depth of the pneumatic injection. A 35-year-old man received a pneumatic injection of the mixed solution (1 mL HA and 9 mL 20% glucose solution) on his forearm, and the specimen taken immediately after the injection were stained with hematoxylin and eosin. (Upper) With 50% pressure power and 0.15 mL volume per shot, the solution (black arrow heads) was laterally dispersed in the whole dermis (scale bars = 500 μm). (Lower) With 85% pressure power and 0.08 mL volume per shot, the solution (*) reached to the subcutis forming larger and fewer droplets, indicating deeper penetration of the solution (scale bars = 500 μm).

high tonicity of the glucose solution enhances the inflammatory response, and hence, wound healing cascade. With the injection system, the operator can select these treatment parameters: injection volume and pressure power.

The pneumatic injections were applied at 5 target sites: 4 along the temporal hairline (preauricular along the zygomatic arch, supra-auricular, temporal along the hairline, and temporal within the main hair mass) and 1 at the malar prominence, with the aim of tightening and contracting the subcutaneous layer such as superficial musculoaponeurotic system (Figure 1). The treatment parameters were set to a "1-shot volume" of 0.08 mL and "pressure power" of 85%, smaller 1-shot volume and higher pressure than those used in previous studies.[1–4] These parameters were specifically chosen to promote penetration into the deeper layers, based on findings from the preliminary experimental study (Figure 2). Thirty consecutive Japanese patients, aged from 41 to 69 years, underwent 3 sessions of treatment at 4-week intervals. The patients with a history of facial rejuvenation treatments in the previous 3 years were excluded.

Clinical outcomes were objectively assessed by comparing photographs taken before, 1 month, and 6 months after the final treatment. As a result, more than half of the patients showed mild to

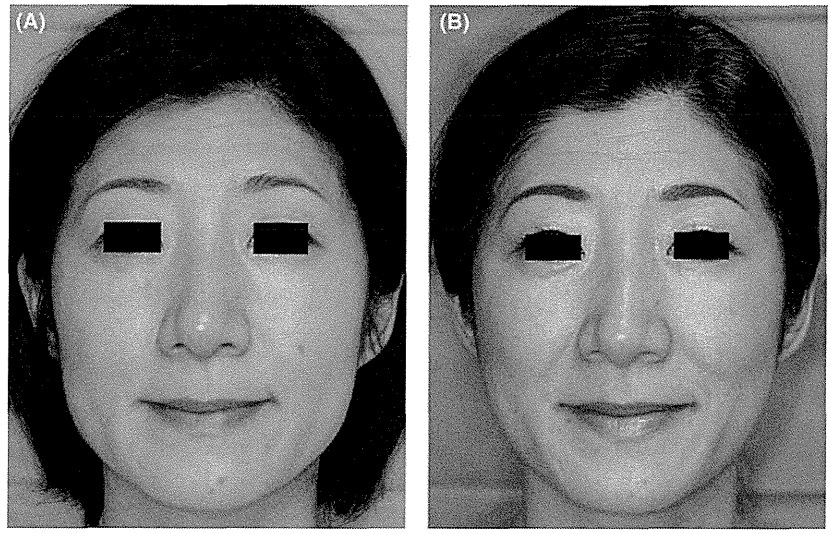

Figure 3. Photographic images of a representative case. This 45-year-old woman underwent 3 sessions of treatment. (A) Preoperative view. (B) View at 1 month after the last treatment.

moderate improvement in aging face, especially in the lower face: jawline and marionette lines (Figure 3). However, aesthetic improvement obtained in this treatment was substantially less than that seen with surgical face-lifts, and partial loss of correction over time was observed in comparison of 1- and 6- month follow-up. It is presumably because the effects due to tissue alteration such as the collagen remodeling persisted for a few months and gradually disappeared over the following months.

Also, patients' self-assessment of the overall appearance of the entire face was conducted at 6-month follow-up after the final treatment. Most of the patients were satisfied with the treatment, suggesting the stretched feeling of the facial skin, which was difficult to detect with photographic assessment. They also reported that the stretched feeling occurred 1 to 2 weeks after each treatment, indicating completion of the inflammatory phase and beginning of the proliferative phase in which wound contraction occurs. The mean pain score using visual analog scale (VAS) was 2.0. No serious complications (e.g., intense postoperative pain, local irritation, persistent erythema, apparent bruising, nerve injury, skin necrosis, or foreign body reaction) occurred, except postinflammatory hyperpigmentation (PIH) in the malar prominence in 2 patients.

Discussion

The authors performed 2 modifications of the pneumatic technology procedures used in previous studies of dermal remodeling treatment: (1) refining the treatment parameters to enable deeper penetration and (2) using hypertonic 20% glucose solution to enhance the inflammatory response. Similar mechanism of high tonicity has been proposed for prolotherapy,[5] and hypertonic stimulation in the treatment remained within the bounds of safety as indicated by the mild VAS pain scores and the absence of serious complications.

A variety of therapeutic modalities for facial rejuvenation are available now, and such techniques as lasers, intense pulsed light, radiofrequency, and ultrasound use the concept of thermal tissue injury to accelerate the wound healing process. However, deep penetration of thermal damage is inevitably accompanied by adverse skin effects such as burns and long-lasting PIH, especially in Asian patients. Thus, the effectiveness of pneumatic injection through tiny openings holds the possibility of surpassing these heat-induced techniques by directly applying stimuli to the subcutaneous tissues, although further modifications are needed.

The results of 30 cases suggested the potential of pneumatic injection of non–cross-linked HA and

hypertonic glucose solution as a novel facial rejuvenation treatment with minimal morbidity and little patient discomfort. The main limitation of this study is the lack of a control group, and the authors cannot conclude whether the aesthetic outcomes originated from the HA, 20% glucose solution, the pneumatic pressure system, or all. However, this is a pilot study that sought to investigate the application of pneumatic pressure system to facial rejuvenation, and further studies are required to optimize the treatment protocol including the placement of injections and the solution component.

Acknowledgments The authors thank Dr. Munehiro Yokoyama for pathological analysis.

References

1. Han TY, Lee JW, Lee JH, Son SJ, et al. Subdermal minimal surgery with hyaluronic acid as an effective treatment for neck wrinkles. Dermatol Surg 2011;37:1291–6.
2. Kim HK, Park MK, Kim BJ, Kim MN, et al. The treatment of keloids with pneumatic technology: a pilot study. Int J Dermatol 2012;51:1502–7.
3. Lee JW, Kim BJ, Kim MN, Lee CK. Treatment of acne scars using subdermal minimal surgery technology. Dermatol Surg 2010;36: 1281–7.
4. Kim BJ, Yoo KH, Kim MN. Successful treatment of depressed scars of the forehead secondary to herpes zoster using subdermal minimal surgery technology. Dermatol Surg 2009;35:1439–40.
5. Rabago D, Best TM, Zgierska AE, Zeisig E, et al. A systematic review of four injections therapies for lateral epicondylosis: prolotherapy, polidocanol, whole blood, and platelet-rich plasma. Br J Sports Med 2009;43:471–81.

TAKANOBU MASHIKO, MD
Department of Plastic Surgery
School of Medicine, University of Tokyo
Tokyo, Japan

YOSHIHISA ABO, MD
Department of Surgery
North Aoyama D Clinic
Tokyo, Japan

SHINICHIRO KUNO, MD
KOTARO YOSHIMURA, MD
Department of Plastic Surgery
School of Medicine, University of Tokyo
Tokyo, Japan

The authors have indicated no significant interest with commercial supporters.

Laser Skin Resurfacing During Isotretinoin Therapy

It is believed that laser procedures should not be performed until 6 to 12 months after the completion of isotretinoin/Accutane therapy. Published studies suggest that laser hair removal with a diode laser, an intense pulsed light, and a neodymium-doped yttrium aluminum garnet (Nd:YAG) laser is safe in patients during treatment with isotretinoin.[1–4] Yoon and colleagues published their data, where they treated 35 patients with acne scars using a 1,550-nm fractional laser. All subjects were started on isotretinoin 10 mg/d for more than 1 month before the laser treatment. None of these patients developed scars.[5] The experiment described here is an attempt to start exploring the possibility of treating acne scars with lasers while patients are on isotretinoin.

Materials and Methods

In a 19-year-old man in his fourth month of treatment at a 40 mg twice a day dose of isotretinoin, 3 sites were marked on the lower back. One site was treated with a nonablative fractional laser, one with ablative fractional laser, and the third with full ablative laser. The nonablative fractional site was treated with 100 mJ/mB, 10-mm spot, 15 milliseconds, 3 passes using a diode 1,540-nm laser. The ablative fractional site was treated with 91 J/cm^2, rep rate of 30 Hz, 3 passes using an erbium:YAG 2,940-nm laser. The full ablative site was treated at 2 J, 5-mm spot, 8 Hz, 8 passes using an erbium:YAG 2,940-nm laser. A 4-mm punch biopsy was performed at each treatment site at each follow-up visit.

Results

At 6-month follow-up visit, nonablative fractional and ablative fractional treated sites showed normal appearing skin with mildly erythematous scars at the biopsy sites, whereas full ablative laser treatment site

Short Communication

For reprint orders, please contact: reprints@futuremedicine.com

Regenerative Medicine

Micronized cellular adipose matrix as a therapeutic injectable for diabetic ulcer

Background: Despite the clinical potential of adipose-derived stem/stromal cells (ASCs), there are some clinical difficulties due to the regulation of cell therapies. **Materials & methods:** Micronized cellular adipose matrix (MCAM) injectable was prepared through selective extraction of connective tissue fractions in fat tissue only through mechanical minimal manipulation procedures. **Results:** It retained some capillaries and ASCs, but most adipocytes were removed. The presence of viable ASCs, vascular endothelial cells was confirmed and ASCs of MCAM kept intact mesenchymal differentiation capacity. In diabetic mice, skin wounds treated with MCAM showed significantly accelerated healing compared with phosphate-buffered saline-treated ones. **Conclusion:** The proven potential of MCAM to accelerate healing in ischemic diabetic ulcers may offer a simple, safe and minimally invasive means for tissue repair and revitalization.

Keywords: adipose stem cells • diabetic ulcer • extracellular matrix • flow cytometry • ischemia • lipoaspirates • minimal manipulation • tissue revitalization • vascular endothelial cells • wound healing

Jingwei Feng‡,1, Kentaro Doi‡,1, Shinichiro Kuno1, Kazuhide Mineda1, Harunosuke Kato1, Kahori Kinoshita1, Koji Kanayama1, Takanobu Mashiko1 & Kotaro Yoshimura*,1

1Departments of Plastic Surgery, University of Tokyo Graduate School of Medicine, 7-3-1, Hongo, Bunkyo-Ku, Tokyo 113-8655, Japan

*Author for correspondence:
Tel: +81 3 5800 8948
Fax: +81 3 5800 8947
kotaro-yoshimura@umin.ac.jp

‡Authors contributed equally

Adipose tissue is structurally complex, harboring a variety of cells within its lobulated fibrous septal network. Through enzymatic digestion, this network can be disintegrated and its heterogeneous complement of indigenous cells, or so called stromal vascular fraction (SVF), may be isolated. Because adipose-derived stem/stromal cells (ASCs) are important SVF residents with mesenchymal multipotency [1,2], SVF has been strategically engaged as a supplement to enhance fat engraftment [1,3–4]. However, if dissociated SVF cells are injected separately, rather than properly integrated into grafted fat, unexpected migratory and/or phenotypic outcomes may result, creating adverse complications (i.e., ectopic fibrosis and lymphadenopathy) [5]. Currently, a number of vehicles for delivery of cells are available, such as injectable biomaterial scaffolds, 3D spheroidal cell cultures and engineered cell sheets [6–8]. These sophisticated constructs help prevent untoward cell migration, thus avoiding lost or undesired contributions by cellular and extracellular matrix (ECM) componentry.

Decellularized ECM of various tissues or organs may serve as bioactive scaffolding, thereby facilitating tissue remodeling and repair [9–11]. Although adipocytes account for >90% of fatty tissue by volume, the native ECM of fat provides a niche for other cellular subsets (e.g., ASCs, vascular endothelial cells and pericytes), enabling biologic functions that are shared in part with acellular dermal matrix.

As niche components, stem cells generally lie in wait for changes in microenvironment. Stem cells isolated from the tissue, however, are already activated in an unphysiological microenvironment, and thus extra care needs to be taken in controlling the fate and behaviors of those cells in clinical utilization. Since 2005, policies of the US FDA aimed at preventing potential contamination and genetic alteration of

Future Medicine part of fsg

stem cells [12] and enzymatic isolation and cultural expansion of ASCs were not considered as 'minimal manipulation', although isolated or cultured ASCs are already extensively used in a number of clinical trials.

For this investigation, a bioactive injectable comprised of functional ECM and resident cells (including ASCs) was formulated through minimal manipulation of adipose tissue. Given the combination of micronized connective tissue, viable ASCs and vascular endothelial cells generated, we have applied the term micronized cellular adipose matrix (MCAM). In this study, injectable MCAM was tested for its therapeutic value for wound repair of diabetic skin ulcer. Wound healing impairment in diabetic patients is a significant clinical issue affecting millions of patients worldwide. The major underlying pathology is noted to be chronic inflammation and ischemia based on peripheral vascular dysfunction, where tissue-resident stem cells are considered to be depleted. Although numerous products for wound dressing with bioactive ECM or growth factors are available, the clinical effects on diabetic ulcer are very limited. Thus, we sought to characterize and evaluate MCAM, which contains human adipose derived stem cells and vascular endothelial cells in their original niche of ECM, as a potential therapeutic tool for stem cell-depleted pathological conditions.

Materials & methods

Mouse tissue preparation

C57BL/6JJcL mouse inguinal fat pads were harvested, washed and weighed. One gram of fat pads was cut into tiny pieces with surgical scissors (continuous fine mincing for 5 min). After transfer to a tube containing 2.5 ml cooled phosphate-buffered saline (PBS), the morcellated tissue was thoroughly shaken several times and then centrifuged (800 × *g*, 5 min). MCAM was extracted as tissue sediment, and floating fatty tissue was also sampled.

Human tissue preparation

Lipoaspirate was obtained from a healthy 23-year-old female donor (BMI = 24) submitting to abdominal liposuction under general anesthesia. The study protocol was approved by our Institutional Review Board. Once soft tissues were infiltrated with a solution of saline plus epinephrine (1:1,000,000), subcutaneous fat was suctioned (-500 to -700 mmHg) using a conventional liposuction machine equipped with a 2.5-mm (inner diameter) cannula. MCAM was extracted from the lipoaspirate with the above described micronization and centrifugation, and floating fat was also sampled.

Whole-mount staining

Whole-mount staining was performed with Wheat germ agglutinin (WGA) Alexa Fluor 488 (Life Technologies, CA, USA), lectin PNA Alexa Fluor 594 (Life Technologies) and Hoechst 33342 solution (Dojindo, Kumamoto, Japan) as instructed by manufacturers. Images were then acquired via confocal microscope (Leica DMIRE2; Leica Microsystems, Wetzlar, Germany).

Flow cytometry

Mouse MCAM and roughly excised inguinal fat were separately prepared. Each sample was digested in 0.1% collagenase (Wako, Osaka, Japan) Hank's balanced salt solution (HBSS) by incubation in a shaking water bath (37°C, 30 min). To remove the collagenase, SVF cells were washed with PBS for three-times. After filtration, SVF cells were washed and stained with the following antibodies and corresponding isotype controls: Anti-CD45-Viogreen (Miltenyi Biotec, Bergisch Gladbach, Germany), Anti-CD34-Biotin (eBioscience, Inc., CA, USA), Rat IgG2a Kappa Control Biotin (BD Biosciences, CA, USA), Streptavidin-APC (BD Biosciences), Anti-CD31-PE (BD Biosciences), Rat IgG2a Kappa Control PE (BD Biosciences). Samples and controls were then analyzed by flow cytometry (MACSQuant Analyzer 10; Miltenyi Biotec). Gating for each signal was set to eliminate 99.9% of the cells in corresponding isotype control. CD45 gating was applied first, and CD45-negative portion was further analyzed for CD34 and CD31 signals.

Cultured ASCs of human origin

Human ASCs in floating fat and in MCAM were cultured separately. Floating fat was digested with collagenase (as above) [12], and isolated SVF cells were seeded in Dulbecco's Modified Eagle Media (DMEM), supplemented with 10% fetal bovine serum (FBS), 100 IU penicillin and 100 mg/ml streptomycin. Explant culture was performed for human MCAM to generate MCAM-derived ASCs.

Multilineage differentiation assay

Assays of adipogenic, osteogenic and chondrogenic lineages were conducted as follows: adipogenic differentiation: ASCs were incubated for 21 days in DMEM containing 10% FBS, 0.5 mM isobutyl-methyl-xanthine, 1 M dexamethasone, 10 µM insulin and 200 µM indomethacin; osteogenic differentiation: ASCs were incubated for 21 days in DMEM containing 10% FBS supplemented with 0.1 mM dexamethasone, 50 mM ascorbate-2-phosphate and 10 mM glycerophosphate (Nacalai Tesque Inc, Kyoto, Japan); and chondrogenic differentiation: a micromass culture system was